Residence Times of the Buried Water Molecules in Bovine Pancreatic Trypsin Inhibitor and Its G36S Mutant[†]

Vladimir P. Denisov,*[,‡] Bertil Halle,[‡] Jörg Peters,[§] and Hans Dietrich Hörlein[§]

Condensed Matter Magnetic Resonance Group, Lund University, Chemical Center, P.O. Box 124, S-22100 Lund, Sweden, and Bayer AG, Verfahrensentwicklung Biotechnologie, D-42096 Wuppertal, Germany

ABSTRACT: The three-dimensional structure of the bovine pancreatic trypsin inhibitor (BPTI) contains 4 internal water molecules, denoted W111, W112, W113, and W122, the latter being replaced by a seryl side chain in the BPTI(G36S) analogue. To investigate the effect of the exchange between these explicit water sites and the bulk solvent, we have measured water ^{17}O and ^2H nuclear magnetic relaxation in solutions of BPTI and the G36S mutant over the Larmor frequency range 2.6–49 MHz. A comparison of the data from the two nuclei shows unequivocally that the isolated buried water molecule, W122, of BPTI contributes only to ^2H, but not to ^{17}O relaxation, while the other 3 waters contribute fully to the relaxation of both nuclei. This demonstrates that the residence time of W122 is in the range 10–200 μs, while the residence times of W111–W113 are in the range 15 ns–1 μs. The slower exchange of W122 indicates that the functionally active region of BPTI, near the Cys14–Cys38 disulfide bond, is less flexible than the central region of BPTI, where the other 3 buried waters are located.

Buried water molecules constitute a highly conserved, integral part of the three-dimensional structure of most globular proteins (Finney, 1979; Edsall & McKenzie, 1983; Baker & Hubbard, 1984; Rashin et al., 1986; Williams et al., 1994) and may contribute significantly to protein stability and function (Meyer, 1992). We have recently shown that buried water molecules are responsible for the water nuclear magnetic relaxation dispersion (NMRD)[1] from protein solutions (Denisov & Halle, 1994, 1995a,b). These NMRD studies have provided the most precise estimates so far available of the residence times of buried water molecules. Since the rate of exchange of buried water molecules with bulk solvent should be limited by conformational fluctuations, water NMRD studies can thus provide information about internal protein dynamics on the nanosecond–millisecond time scale. Although this is in the time scale of many biofunctionally related processes, it can be accessed by few other techniques (Lane & Lefévre, 1994). While similar in spirit to the classical hydrogen exchange method (Wagner, 1983; Englander & Kallenbach, 1984), the water NMRD technique yields information more closely related to protein dynamics, since, unlike the covalently attached hydrogens, the exchange rate of buried water molecules is limited by conformational fluctuations.

The crystal structure of the 58-residue protein bovine pancreatic trypsin inhibitor (BPTI) contains 4 buried water molecules in all 3 investigated crystal forms (Deisenhofer

& Steigemann, 1975; Wlodawer et al., 1984, 1987a,b). These water molecules are found at the same positions in the solution structure (Otting & Wüthrich, 1989), which is virtually identical to the crystal structure (Berndt et al., 1992). The locations of the 4 buried water molecules in BPTI are shown in Figure 1. The water molecule denoted W122 is buried in small cavity between the loop segments comprising residues 11–14 and 36–38, forming two hydrogen bonds to each loop. The water oxygen is located 4 Å from the center of the Cys14–Cys38 disulfide bond. W122 resides in the region of the BPTI molecule that associates tightly with the active site of serine proteases (Rühlmann et al., 1973). The remaining 3 water molecules, denoted W111–W113, reside in a pore-like cavity where they hydrogen bond to each other and to residues in the loop segments 7–10 and 41–44. W111 occupies the mouth of the cavity, but is not hydrogen-bonded to external water. The most deeply buried water molecule, W113, is located 7 Å from the isolated water molecule W122.

An ^{18}O gel filtration study showed that the buried water molecules in BPTI exchange with bulk water within the experimental dead time of ca. 15 s (Tüchsen et al., 1987). Multidimensional NMR studies subsequently confined the residence times of these buried water molecules to the range 0.3 ns–20 ms at 4 °C (Otting et al., 1991a,b). The residence time range was further narrowed down by our recent water ^{17}O NMRD study to 7 ns–4 μs at 27 °C for at least 2, more probably 3, of the 4 buried water molecules (Denisov & Halle, 1995a). The water ^2H NMRD data indicate that the fourth buried water molecule has a residence time in the range 4–200 μs, too long to contribute to the rapid ^{17}O relaxation (Denisov & Halle, 1995b).

While the water NMRD technique provides direct dynamic information in the frequency domain, it does not, like high-resolution multidimensional NMR, provide spatial resolution. Nevertheless, by modifying a protein and recording the effect on the dispersion profile, one can, in favorable cases, monitor

---

[1] Abbreviations: BPTI, bovine pancreatic trypsin inhibitor; BPTI-(G36S), BPTI mutant with Gly36 replaced by Ser; SDS, sodium dodecyl sulfate; PAGE, polyacrylamide gel electrophoresis; RP-HPLC, reverse-phase high-performance liquid chromatography; NMR, nuclear magnetic resonance; NMRD, nuclear magnetic relaxation dispersion.
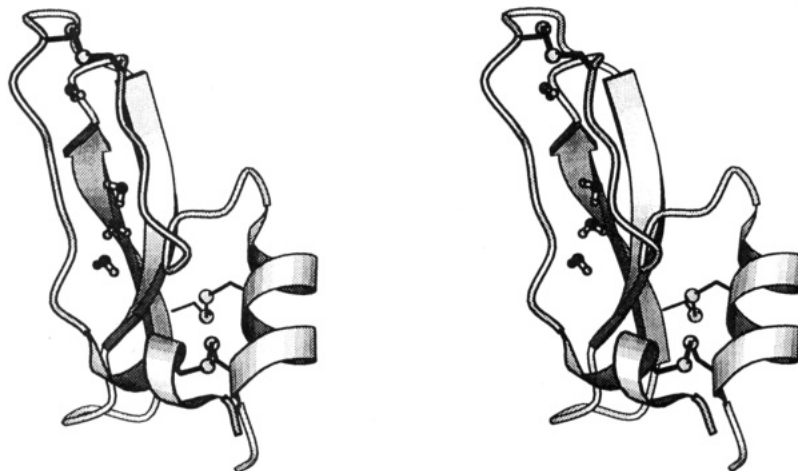
FIGURE 1: Stereoview of the backbone fold in the crystal structure of BPTI (Wlodawer et al., 1987a; PDB file 5PTI), showing the location of the 4 buried water molecules (W122 at the top) and the 3 disulfide bonds. The drawing was made with the program Molscript (Kraulis, 1991).

individual water molecules also by the NMRD technique. This is illustrated by the present water NMRD study of wild-type and mutant forms of BPTI.

The G36S mutant differs from wild-type BPTI by the replacement of Gly36 by Ser and by the addition of a methionine residue at the N-terminus. The BPTI(G36S) mutant has recently been studied by high-resolution ^{1}H NMR, showing that the backbone conformation and hydrogen-bond network are virtually the same as in wild-type BPTI except in the immediate vicinity of the mutation site (Berndt et al., 1993; Otting et al., 1993). The only major difference between the two protein structures is that the buried water molecule W122 in BPTI is replaced by the hydroxyl group of Ser36 in BPTI(G36S) (Berndt et al., 1993); cf. Figure 2. A comparison of the water ^{2}H and ^{17}O NMRD profiles from BPTI with the corresponding dispersion profiles from BPTI-(G36S) should thus allow us to isolate the contribution to the observed bulk water relaxation from the buried water molecule W122.

We report here that the removal of W122 has a negligible effect on the [17]O dispersion profile, whereas the amplitude of the ^{2}H dispersion step is considerably reduced. This finding unambiguously demonstrates that the buried water molecule W122 in BPTI has a residence time in the range 10−200 μs, at least an order of magnitude longer than for the other 3 buried water molecules. Furthermore, the finding that the exchange of the completely buried W122 is at least 3 orders of magnitude faster than localized atomic rear-rangements in its vicinity, such as the aromatic ring flipping of Tyr35, and the isomerization of the 14−38 disulfide bond (Wagner, 1983; Otting et al., 1993; Szyperski et al., 1993) demonstrates that the latter motions are not correlated with the (much faster) conformational fluctuations that provide the escape route for W122.

MATERIALS AND METHODS

Materials. The BPTI(G36S) recombinant mutant was prepared as described elsewhere (Berndt et al., 1993). The mutant and wild-type proteins were subjected to the same purification steps and were lyophilized as salts of trifluoro-acetic acid. The purity of both protein preparations was 99.7% according to SDS−PAGE and RP-HPLC.

Protein solutions were made by dissolving the lyophilized proteins in heavy water (molar mass 21.5 g mol^{−1}), enriched
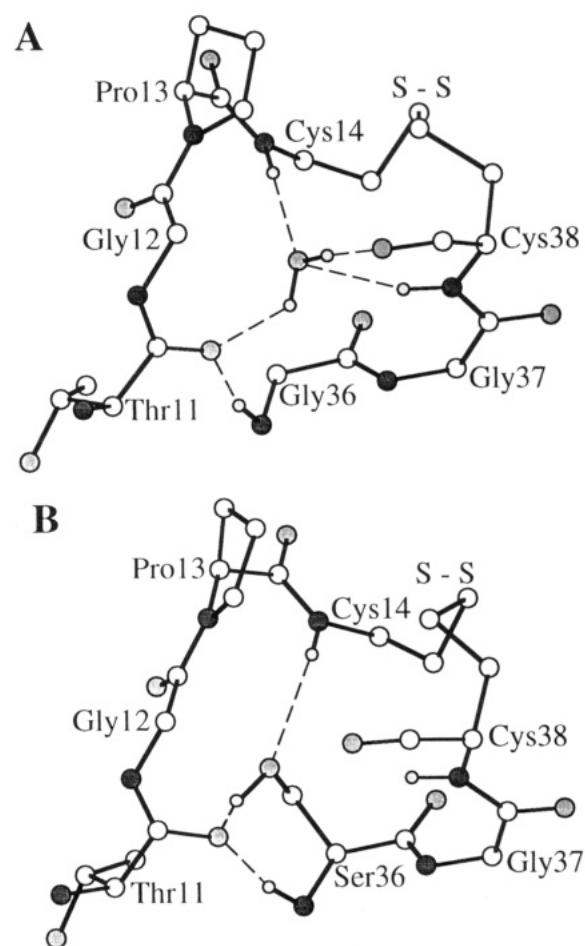

FIGURE 2: (A) Hydrogen bonding of the internal water molecule W122 in BPTI (Wlodawer et al., 1987a; Protein Data Bank, file 5PTI). Only hydrogen atoms that participate in hydrogen bonds are shown. (B) Same representation of the corresponding region in BPTI(G36S), where the hydroxyl group of Ser36 replaces W122. This picture was constructed with the program MacMimic, using the crystal structure coordinates of BPTI, as in (A), and with the geometry of the Ser36 residue according to the NMR solution structure (Berndt et al., 1993).

in [17]O (Ventron, 21.9 atom % [17]O, 61.9 atom % [18]O, 99.95 atom % [2]H). pH was measured with a Radiometer PHM63 digital pH-meter equipped with a 5-mm combination elec-trode. The direct reading pH* from a D₂O solution (with

the pH-meter calibrated with standard H_2O buffers) was converted to thermodynamically meaningful pD values according to pD = pH* + 0.41 (Covington et al., 1968). Both proteins were studied at pD 5.6, adjusted by adding small amounts of 5 M KOH to the protein solutions.

Protein concentrations were determined by complete amino acid analysis, which also confirmed the high purity of the protein preparations (cf. above). The concentrations obtained in this way were 25.7 ± 0.4 mM (14.1 ± 0.2 wt %) for wild-type BPTI, and 22.7 ± 0.4 mM (12.7 ± 0.2 wt %) for the G36S mutant. In addition, the protein solutions contained up to 0.5 M trifluoroacetate.

Relaxation Dispersion Measurements. Oxygen-17 and deuteron relaxation rates were measured at eight magnetic field strengths: at 7.0 T on a Varian Unity 300 spectrometer, at 4.7 T on a Bruker DMX 200 spectrometer, at 2.35 T on a Bruker MSL 100 spectrometer, and at 1.83, 1.505, 1.05, 0.7, and 0.45 T using an iron magnet (Drusch EAR-35N) equipped with field-variable lock and flux stabilizer and operated from the MSL 100 spectrometer. The sample temperature was maintained at 27.0 ± 0.1 °C by a thermostated air flow.

The longitudinal and transverse relaxation rates were measured as described elsewhere (Denisov & Halle, 1995a,b).

RESULTS AND DISCUSSION

Spin Relaxation Dispersion from Protein Solutions. The longitudinal relaxation of water ^{17}O and ^2H nuclei in aqueous protein solutions is known to exhibit a dispersion in the megahertz range. The observation that the inflection frequency for both nuclei reflects the rotational correlation time, τ_R, of the protein shows that some water molecules are associated with the protein for a period long compared to τ_R (Koenig et al., 1975; Halle et al., 1981). We have recently demonstrated that only the 4 buried water molecules in BPTI are sufficiently long-lived to contribute to the relaxation dispersion (Denisov & Halle, 1994, 1995a,b). A quantitative comparison of ^{17}O and ^2H relaxation rates from protein solutions is possible, since both rates reflect fluctuations of the electric quadrupole interaction of nuclei residing in exchanging water molecules (Halle & Wennerström, 1981a). Although ^2H relaxation rates may be significantly influenced by deuteron exchange between water and labile protein hydrogens (Piculell & Halle, 1986; Hills et al., 1989; Hills, 1992), this contribution is negligible in BPTI solutions around pD 5.5 (Denisov & Halle, 1995b).

Figures 3 and 4 show the ^{17}O and ^2H relaxation dispersion profiles from solutions of BPTI and BPTI(G36S) at pD 5.6. The data are accurately represented by the standard theoretical expression (Abragam, 1961; Halle & Wennerström, 1981b)

$$R_1(\omega_0) = R_{hf} + \beta\tau_c\left[\frac{0.2}{1 + (\omega_0\tau_c)^2} + \frac{0.8}{1 + (2\omega_0\tau_c)^2}\right] \quad (1)$$

where ω_0 is the Larmor frequency and τ_c is the effective correlation time for the long-lived water molecules, usually identified with the rotational correlation time, τ_R, of the protein. The dispersion amplitude β is due to buried water molecules, while the frequency relaxation rate $R_{hf} \equiv R_1(\omega_0 \gg 1/\tau_c)$ contains the contributions from all other water molecules in the bulk and at the protein surface. The
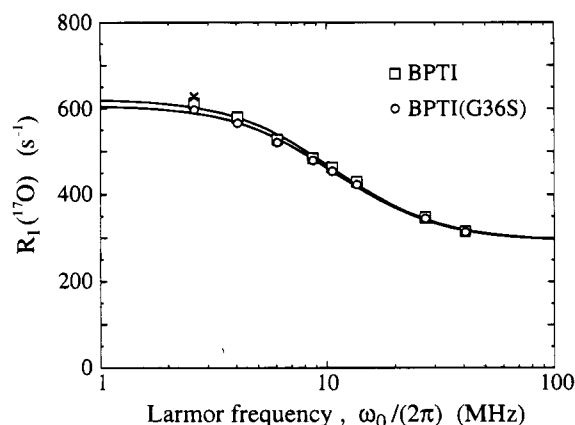
FIGURE 3: Dispersion of water ^{17}O longitudinal relaxation rate in D_2O solutions (27 °C, pD 5.6) of BPTI and BPTI(G36S). The original BPTI(G36S) data are shown, while the BPTI data were scaled to the same concentration and molecular mass as for BPTI-(G36S), assuming that the excess relaxation rate $(R_1 - R_{bulk})$ is proportional to $w/(1 - w)/M_P$ (cf. eqs 1 and 2). The small (ca. 5%) increase of R_{bulk} due to trifluoroacetate has a negligible effect on this scaling. The estimated error bars for R_1 are of the same size as the data symbols. The curves resulted from a fit of the parameters R_{hf}, β, and τ_c in eq 1 to the eight data points. The single R_2 value for BPTI(G36S) at the lowest field is indicated by a cross.
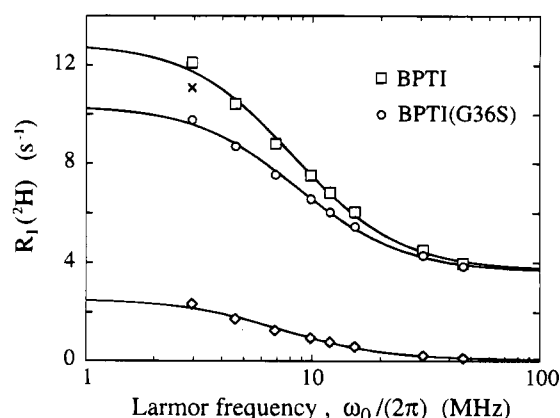
FIGURE 4: Dispersion of water ^2H longitudinal relaxation rate in D_2O solutions (27 °C, pD 5.6) of BPTI and BPTI(G36S). The original BPTI(G36S) data are shown, while the BPTI data were scaled in the same way as in Figure 3. The estimated error bars for R_1 are of the same size as the data symbols. The curves resulted from a fit of the parameters R_{hf}, β, and τ_c in eq 1 to the eight data points. The single R_2 value for BPTI(G36S) at the lowest field is indicated by a cross. At the bottom, the difference between the two upper sets of data is shown.

Table 1: Parameters Derived from Fits to ^{17}O and ^2H NMRD Data (Unscaled) from BPTI and BPTI(G36S) Solutions

protein	R_{hf}, s^{-1}	β, 10^9s^{-2}	τ_c, ns
	^{17}O		
BPTI	312 ± 4	45.3 ± 1.5	8.4 ± 0.3
BPTI(G36S)	292 ± 4	38.0 ± 1.5	8.3 ± 0.3
	^2H		
BPTI	3.95 ± 0.04	0.964 ± 0.015	11.0 ± 0.3
BPTI(G36S)	3.66 ± 0.04	0.638 ± 0.015	10.5 ± 0.3

parameters R_{hf}, β, and τ_c, determined from nonlinear least-squares fits to the eight data points, are given in Table 1. For both nuclei, the transverse relaxation rate, R_2, was measured at the lowest frequency to exclude the possibility of a further dispersion step below 2 MHz. Taking into account the small frequency-independent contribution to R_2 from scalar relaxation, which is completely negligible only

at pD <3 (Halle & Karlström, 1983; Denisov & Halle, 1995a,b), the R_2 data in Figures 3 and 4 demonstrate that the observed leveling off of R_1 at low frequencies really defines the zero-frequency plateau, where R_1 is equal to $R_2 - R_2^{scalar}$.

Residence Times of Buried Water Molecules. Figures 3 and 4 show that the removal of the buried water molecule W122 reduces the amplitude of the ^{2}H relaxation dispersion step by ca. 20% without significantly affecting the ^{17}O relaxation dispersion. This finding conclusively demonstrates that W122 is the most slowly exchanging of the 4 buried water molecules in BPTI, as previously hypothesized (Denisov & Halle, 1995a,b).

For a water molecule, trapped inside the protein, to contribute to the spin relaxation of solvent nuclei, its mean residence time, τ_{res}, must obey the inequalities: $\tau_R < \tau_{res} < T_I$. The intrinsic (zero-frequency) relaxation time T_I ($=1/R_I$) for a water molecule in a protein with rotational correlation time $\tau_R = 10$ ns is approximately 200 μs for ^{2}H and 4 μs for ^{17}O (Denisov & Halle, 1995b). The fast-exchange condition $\tau_{res} < T_I$ is thus considerably less restrictive for ^{2}H than for ^{17}O relaxation. For W122 to contribute only to the ^{2}H relaxation, its residence time must be in the range $T_I(^{17}$O$) < \tau_{res} < T_I(^2$H$)$. Actually, τ_{res} must be considerably larger than $T_I(^{17}$O$)$, since the ^{17}O dispersion curves for BPTI and BPTI(G36S) in Figure 3 coincide within the experimental uncertainty. (Roughly half of the, not statistically significant, difference between the fitted dispersion profiles in Figure 3 can be accounted for by the 1% difference in the correlation times; cf. Table 1.) We can thus conclude that the residence time of W122 in BPTI is in the range 10–200 μs. The ^{17}O dispersion is due to W111–W113, which thus have residence times in the range 10 ns–4 μs.

Before comparing the ^{2}H and ^{17}O dispersion amplitudes β, we note that the τ_c values obtained from the ^{17}O and ^{2}H fits are slightly different (cf. Table 1), although there is no doubt that both $\tau_c(^{17}$O$)$ and $\tau_c(^2$H$)$ mainly reflect the rotational diffusion of BPTI molecules. This difference, also seen in our previous studies of BPTI, cannot be explained by the nonspherical hydrodynamic shape of the BPTI molecule (Denisov & Halle, 1995a). While a residence time close to $T_I(^{17}$O$)$ could explain the observation $\tau_c(^{17}$O$) < \tau_c(^2$H$)$, the quantitative scaling of the ^{17}O and ^{2}H data for BPTI(G36S) seems to rule out this possibility (cf. below). A systematic error in the relaxation measurements is also an unlikely cause of the difference, since it was not seen in similar studies of several other proteins (Denisov and Halle, unpublished results). Finally, we note that the ca. 25% increase in τ_c with respect to our previous study of 19 mM BPTI can be ascribed to the 35% higher concentration used here and to the slightly larger solvent viscosity due to trifluoroacetate. Since $\tau_c = (1/\tau_{res} + 1/\tau_R)^{-1}$ is not significantly shorter than the expected τ_R, we can raise the lower bound for τ_{res} of W111–113 to, say, 15 ns. For example, if these 3 waters had $\tau_{res} = \tau_R$, the correlation time τ_c deduced from the dispersions would imply a rotational correlation time of $\tau_R = 2\tau_c \approx 20$ ns, which is definitely too large.

The Number of Buried Water Molecules and Their Order Parameters. To check that the ^{2}H and ^{17}O relaxation dispersions from BPTI(G36S) really monitor the same number of buried water molecules, we now compare the dispersion amplitudes. The amplitude of the low-frequency

relaxation dispersion, as measured by the parameter β, is related to the protein mass fraction, w, and the number, N_I, of long-lived ($\tau_{res} \gg \tau_R$) water molecules per protein molecule (Denisov & Halle, 1995a,b):

$$\beta = CN_I A_I^2 \chi_I^2 \frac{M_W w}{M_P(1 - w)} \qquad (2)$$

where C is a spin-dependent factor, equal to $12\pi^2/125$ for ^{17}O and $3\pi^2/2$ for ^{2}H, and M_P and M_W are the molar masses of protein and water, respectively. Further, χ_I is the quadrupole coupling constant and A_I the generalized order parameter (Halle & Wennerström, 1981a) for a nucleus in a buried water molecule. The quantity A_I^2 in eq 2 should be interpreted as an average over the long-lived water molecules (Denisov & Halle, 1995a).

If $\beta(^{17}$O$)$ and $\beta(^2$H$)$ reflect the same number of water molecules, their ratio should be equal to $(8/125)[\chi_I(^{17}$O$)/\chi_I(^2$H$)]^2$ (Denisov & Halle, 1995b). Since the ratio $\chi_I(^{17}$O$)/\chi_I(^2$H$) = 30.5 \pm 1.5$ is remarkably invariant to the local hydrogen-bond environment of a water molecule (Poplett, 1982), we expect that $\beta(^{17}$O$)/\beta(^2$H$) = 60 \pm 6$. For BPTI-(G36S) we obtain 60 ± 4 for this ratio (cf. Table 1), demonstrating that the ^{17}O and ^{2}H dispersions from BPTI-(G36S) are due to the same long-lived water molecules, i.e., the buried waters W111–W113. For BPTI the ratio is 47 ± 3, significantly smaller than the reference value, as indeed expected if the most slowly exchanging W122 contributes only to the ^{2}H relaxation (cf. above).

As argued elsewhere (Denisov & Halle, 1995a), the quadrupole coupling constants for the strongly hydrogen-bonded buried water molecules in BPTI should not deviate much from the values for D$_2$O ice Ih, i.e., $\chi_I(^2$H$) = 213$ kHz and $\chi_I(^{17}$O$) = 6.5$ MHz. From the β value derived from a fit to the difference data in Figure 4 (the bottom curve), we can then, using eq 2, determine the second-rank orientational order parameter for W122: $A_I = 0.82 \pm 0.03$. This is somewhat lower than the value estimated by a comparison of ^{17}O and ^{2}H data, neglecting any librational averaging (Denisov & Halle, 1995b). The present value, resulting from ^{2}H difference data, does not rely on additional assumptions and should thus be more accurate.

For the purpose of directly comparing the ^{17}O and ^{2}H dispersions, it is convenient to scale the measured relaxation rates according to

$$R_1^{scaled} = (R_1(\omega_0) - R_{hf})\frac{M_P(1 - w)}{C\chi_I^2 M_W w \tau_c} =$$

$$N_I A_I^2 \left[\frac{0.2}{1 + (\omega_0\tau_c)^2} + \frac{0.8}{1 + (2\omega_0\tau_c)^2}\right] \qquad (3)$$

where the last result follows from eqs 1 and 2. Adopting the ice values for the quadrupole coupling constants and taking the parameters R_{hf} and τ_c from Table 1, we obtain the scaled dispersion profiles shown in Figure 5 (plotted versus $\omega_0\tau_c$ to remove the effect of the slight difference between the ^{17}O and ^{2}H correlation times). Within experimental error, the two ^{17}O dispersions and the ^{2}H dispersion from BPTI(G36S) coincide, as expected if they are due to the more rapidly exchanging group of buried waters (W111–W113). The residence times for these water molecules must
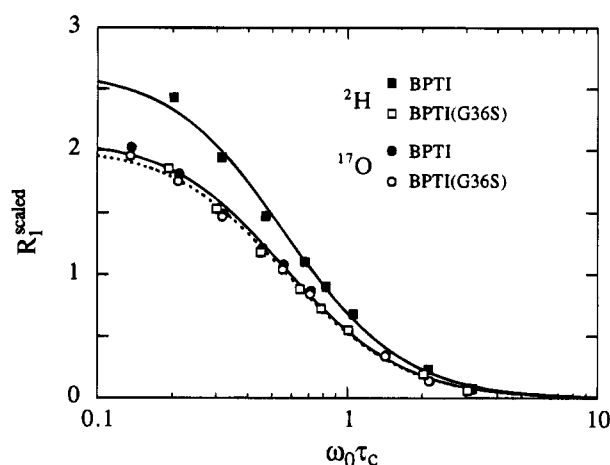
FIGURE 5: The scaled ^2H and ^{17}O relaxation dispersions from D_2O solutions (27 °C, pD 5.6) of BPTI and BPTI(G36S); see eq 3. The original data are taken from Figures 3 and 4. The estimated error bars are of the same size as the data symbols. The four curves (solid for BPTI, dashed for G36S) were scaled in the same way as the data points. (Note that the two dashed curves are nearly superimposed.)

be significantly shorter than $T_1(^{17}O)$, say, $\tau_{res} < 1$ μs; otherwise, the scaled ^{17}O and ^2H dispersions from BPTI-(G36S) would not coincide.

The value $N_1A_1{}^2 = 2.04 \pm 0.04$, obtained from the three coincident curves in Figure 5, is consistent with the previous result $N_1A_1{}^2(^{17}O) = 2.1 \pm 0.1$ (Denisov & Halle, 1995a,b). The present results also show that $N_1A_1{}^2(^{17}O)$ and $N_1A_1{}^2(^2H)$ are equal within experimental error. This might indicate librational averaging of ca. 20° amplitude; in the absence of such averaging, $N_1A_1{}^2(^{17}O) = 1.3N_1A_1{}^2(^2H)$ due to the different orientation of the ^{17}O and ^2H electric field gradient tensors (Denisov & Halle, 1995a). The experimental result, $N_1A_1{}^2 = 2.04$, is consistent with order parameters close to unity, say, $A_1 = 0.9$, for the two most deeply buried waters W112 and W113, and a somewhat smaller order parameter, say, $A_1 = 0.6$, for the water molecule W111 at the mouth of the pore-like cavity.

The Mechanism of Water Exchange. For a buried water molecule to exchange with bulk water, a transient displacement of protein atoms must occur that locally unfolds the native protein conformation or, at least, opens up a channel wide enough to accomodate the exchanging water molecule. The two regions of the BPTI molecule that contain buried water molecules are located between the two extensive loops of the protein backbone (see Figure 1). The finding that W122 exchanges at least an order of magnitude more slowly than W111−W113 indicates that the exchange-limiting conformational fluctuations in these two regions are uncorrelated. The slower exchange of W122 may be related to the presence of the nearby Cys14−Cys38 disulfide bond, which should limit the amplitude of loop fluctuations. In contrast, W111−W113 are far removed from all 3 disulfide bonds.

It is instructive to compare the 10−200 μs residence time of W122 with the time scales of other dynamic processes occurring in its neighborhood. These include 180° flips of the aromatic ring of Tyr35 on a time scale of 1 s at 27 °C and isomerization of the Cys14−Cys38 disulfide bond with a residence time of ca. 0.2 s at 27 °C for the dominant conformer (Otting et al., 1993). Besides local segmental motions of Cys38−Arg39 that correlate well with the latter

isomerization, there are also indications of a faster process, affecting residues 14−16, on the time scale 3 ns−0.1 ms at 36 °C (Szyperski et al., 1993). While the aromatic ring flip and the disulfide bond isomerization are both too slow to be correlated with the exchange of W122, the faster motion of Cys14 may well be directly involved in the exchange mechanism. Although the amides of both Cys14 and Cys38 donate hydrogen bonds to W122, an examination of the crystal structure suggests a likely escape path for W122 via the small opening of the cavity partly blocked by the Cys14 amide.

In BPTI(G36S) the hydroxyl group of Ser36, which replaces W122, is engaged in 2 of the 4 hydrogen bonds attributed to W122 in wild-type BPTI (Berndt et al., 1993). It is noteworthy that the hydroxyl proton resonance of Ser36 was observed separately from the water signal (Berndt et al., 1993), implying slow exchange (residence time $\gg 1$ ms) of this proton with bulk water. As this rate is much slower than the exchange rate of W122 occupying the same position in wild-type BPTI, it should be related to the rupture of the covalent O−H bond rather than to a correspondingly low solvent accessibility of this site. Similarly, amide protons that are hydrogen-bonded to W111−W113 exchange many orders of magnitude more slowly than the buried water molecules (Tüchsen et al., 1987; Denisov & Halle, 1995b).

CONCLUSIONS

The present comparative ^{17}O and ^2H NMRD study of wild-type BPTI and its G36S analogue demonstrates that, among the 4 buried water molecules in BPTI, W122 exchanges much more slowly than the 3 others, with a residence time in the range 10−200 μs. While this exchange rate is fast compared to the intrinsic ^2H relaxation rate, it is much slower than the intrinsic ^{17}O relaxation rate of W122. Consequently, this water molecule contributes to the ^2H, but not to the ^{17}O, spin relaxation dispersion, as clearly shown by the comparison of relaxation data from solutions of BPTI and BPTI-(G36S).

To our knowledge, the data in Figure 4 provide the first observation of a single water molecule in a protein solution by means of the NMRD technique. The magnitude of the W122 contribution to the ^2H relaxation rate yields the order parameter $A_1 = 0.82 \pm 0.03$ for this water molecule. The residence times of W111−W113 fall in the range 15−1000 ns.

The large difference in the exchange rates of W122 and W111−W113 demonstrates that displacements of the protein backbone from its average position are much slower in the active region of BPTI near the 14−38 disulfide bond. More details about the mechanism of buried water exchange can be obtained by temperature-dependent NMRD studies, which are in progress.

The dominant influence of the exchanging buried water molecules on the magnetic relaxation of solvent nuclei makes them useful as intrinsic probes of internal protein dynamics in the biofunctionally important nanosecond−millisecond window, accessible by few other techniques (Lane & Lefévre, 1994).

ACKNOWLEDGMENT

REFERENCES

Abragam, A. (1961) *The Principles of Nuclear Magnetism*, Clarendon Press, Oxford.

Baker, E. N., & Hubbard, R. E. (1984) *Prog. Biophys. Mol. Biol. 44*, 97−179.

Berglund, B., Lindgren, J., & Tegenfeldt, J. (1978) *J. Mol. Struct. 43*, 179−191.

Berndt, K. D., Güntert, P., Orbons, L. P. M., & Wüthrich, K. (1992) *J. Mol. Biol. 227*, 757−775.

Berndt, K. D., Beunink, J., Schröder, W., & Wüthrich, K. (1993) *Biochemistry 32*, 4564−4570.

Covington, A. K., Paabo, M., Robinson, R. A., & Bates, R. G. (1968) *Anal. Chem. 40*, 700−706.

Deisenhofer, J., & Steigemann, W. (1975) *Acta Crystallogr. B 31*, 238−250.

Denisov, V. P., & Halle, B. (1994) *J. Am. Chem. Soc. 116*, 10324−10325.

Denisov, V. P., & Halle, B. (1995a) *J. Mol. Biol. 245*, 682−697.

Denisov, V. P., & Halle, B. (1995b) *J. Mol. Biol. 245*, 698−709.

Edsall, J. T., & McKenzie, H. A. (1983) *Adv. Biophys. 16*, 53−183.

Englander, S. W., & Kallenbach, N. R. (1984) *Q. Rev. Biophys. 16*, 521−655.

Finney, J. L. (1979) in *Water, A Comprehensive Treatise* (Franks, F., Ed.) Vol. 6, Chapter 2, pp 47−122, Plenum Press, New York.

Halle, B., & Wennerström, H. (1981a) *J. Chem. Phys. 75*, 1928−1943.

Halle, B., & Wennerström, H. (1981b) *J. Magn. Reson. 44*, 89−100.

Halle, B., & Karlström, G. (1983) *J. Chem. Soc., Faraday Trans. 2 79*, 1031−1046.

Halle, B., Andersson, T., Forsén, S., & Lindman, B. (1981) *J. Am. Chem. Soc. 103*, 500−508.

Hills, B. P. (1992) *Mol. Phys. 76*, 489−508.

Hills, B. P., Takacs, S. F., & Belton, P. S. (1989) *Mol. Phys. 67*, 903−918.

Koenig, S. H., Hallenga, K., & Shporer, M. (1975) *Proc. Natl. Acad. Sci. U.S.A. 72*, 2667−2671.

Kraulis, P. J. (1991) *J. Appl. Crystallogr. 24*, 946−950.

Lane, A. N., & Lefévre, J.-F. (1994) *Methods Enzymol. 239*, 596−619.

Meyer, E. (1992) *Protein Sci. 1*, 1543−1562.

Otting, G., & Wüthrich, K. (1989) *J. Am. Chem. Soc. 111*, 1871−1875.

Otting, G., Liepinsh, E., & Wüthrich, K. (1991a) *Science 254*, 974−980.

Otting, G., Liepinsh, E., & Wüthrich, K. (1991b) *J. Am. Chem. Soc. 113*, 4363−4364.

Otting, G., Liepinsh, E., & Wüthrich, K. (1993) *Biochemistry 32*, 3571−3582.

Piculell, L., & Halle, B. (1986) *J. Chem. Soc., Faraday Trans. 1 82*, 401−414.

Poplett, I. J. F. (1982) *J. Magn. Reson. 50*, 397−408.

Rashin, A. A., Iofin, M., & Honig, B. (1986) *Biochemistry 25*, 3619−3625.

Rühlmann, A., Kukla, D., Schwager, P., Bartels, K., & Huber, R. (1973) *J. Mol. Biol. 77*, 417−436.

Szyperski, T., Luginbühl, P., Otting, G., Güntert, P., & Wüthrich, K. (1993) *J. Biomol. NMR 3*, 151−164.

Tüchsen, E., Hayes, J. M., Ramaprasad, S., Copie, V., & Woodward, C. (1987) *Biochemistry 26*, 5163−5172.

Wagner, G. (1983) *Q. Rev. Biophys. 16*, 1−57.

Williams, M. A., Goodfellow, J. M., & Thornton, J. M. (1994) *Protein Sci. 3*, 1224−1235.

Wlodawer, A., Walter, J., Huber, R., & Sjölin, L. (1984) *J. Mol. Biol. 180*, 301−329.

Wlodawer, A., Deisenhofer, J., & Huber, R. (1987a) *J. Mol. Biol. 193*, 145−156.

Wlodawer, A., Nachman, J., Gilliland, G. L., Gallagher, W., & Woodward, C. (1987b) *J. Mol. Biol. 198*, 469−480.